AMERICAN SOCIETY FOR MICROBIOLOGY | Infection and Immunity®

MOLECULAR PATHOGENESIS

Borrelia burgdorferi CheY2 Is Dispensable for Chemotaxis or Motility but Crucial for the Infectious Life Cycle of the Spirochete

Hui Xu,[a] Syed Sultan,[a] Aaron Yerke,[a] Ki Hwan Moon,[a] R. Mark Wooten,[b] M. A. Motaleb[a]

Department of Microbiology and Immunology, Brody School of Medicine, East Carolina University, Greenville, North Carolina, USA[a]; Department of Medical Microbiology and Immunology, College of Medicine and Life Sciences, University of Toledo, Toledo, Ohio, USA[b]

ABSTRACT The requirements for bacterial chemotaxis and motility range from dispensable to crucial for host colonization. Even though more than 50% of all sequenced prokaryotic genomes possess at least one chemotaxis signaling system, many of those genomes contain multiple copies of a chemotaxis gene. However, the functions of most of those additional genes are unknown. Most motile bacteria possess at least one CheY response regulator that is typically dedicated to the control of motility and which is usually essential for virulence. *Borrelia burgdorferi* appears to be notably different, in that it has three *cheY* genes, and our current studies on *cheY2* suggests that it has varied effects on different aspects of the natural infection cycle. Mutants deficient in this protein exhibit normal motility and chemotaxis *in vitro* but show reduced virulence in mice. Specifically, the *cheY2* mutants were severely attenuated in murine infection and dissemination to distant tissues after needle inoculation. Moreover, while Δ*cheY2* spirochetes are able to survive normally in the *Ixodes* ticks, mice fed upon by the Δ*cheY2*-infected ticks did not develop a persistent infection in the murine host. Our data suggest that CheY2, despite resembling a typical response regulator, functions distinctively from most other chemotaxis CheY proteins. We propose that CheY2 serves as a regulator for a *B. burgdorferi* virulence determinant that is required for productive infection within vertebrate, but not tick, hosts.

KEYWORDS *Borrelia burgdorferi*, Lyme disease, spirochetes, chemotaxis, response regulator, CheY, virulence, chemotaxis/motility, tick-mouse, flagella, pathogenesis

Received 28 March 2016 **Returned for modification** 5 May 2016 **Accepted** 23 October 2016

Accepted manuscript posted online 31 October 2016

Citation Xu H, Sultan S, Yerke A, Moon KH, Wooten RM, Motaleb MA. 2017. *Borrelia burgdorferi* CheY2 is dispensable for chemotaxis or motility but crucial for the infectious life cycle of the spirochete. Infect Immun 85:e00264-16. https://doi.org/10.1128/IAI.00264-16.

Editor Shelley M. Payne, University of Texas at Austin

Address correspondence to M. A. Motaleb, motalebm@ecu.edu.

Borrelia burgdorferi is the causative organism of Lyme disease, which is the most common vector-borne illness in the United States and Europe (1, 2). During its natural enzootic cycle, the organism must survive within a vertebrate host (usually a rodent) and a tick vector of an *Ixodes* species. Spirochete-infected ticks efficiently transmit the bacteria during a blood meal to the vertebrate host, where the organisms disseminate from the initial site of inoculation in the dermis to several distant tissues, such as tibiotarsal joints, heart, and the nervous system, where they persist to produce various clinical manifestations (3–5). *B. burgdorferi* is a highly motile organism whose motility is provided by flagella that are enclosed by the outer membrane and thus are called periplasmic flagella (6–9). Motility is absolutely required for migration of *B. burgdorferi* from the skin to distant tissues, establishment of persistent infection in mice, transmission from the tick vector to the murine host, and optimal survival in ticks (6, 7, 10). Chemotaxis is also important for the spirochetal infectious life cycle, as these

pathways are involved in directing bacterial motility during the different stages of infection (11–13).

Chemotaxis, which uses a two-component signaling system, has been extensively studied in *Escherichia coli* and *Salmonella enterica* serovar Typhimurium; thus, these organisms serve as model organisms (14–17). In these systems, the two-component system is initiated when a membrane-bound protein, called the methyl-accepting chemotaxis protein (MCP), binds a ligand. This action causes signal transduction from the MCP to a histidine kinase, CheA, via a linker protein known as CheW. CheA autophosphorylates, which then transfers its phosphate to CheY. Phosphorylated CheY in turn binds to the flagellar switch proteins FliM and FliN to alter cellular behavior (18). Binding to the flagellar proteins causes a change in the direction of flagellar rotation from the default counterclockwise (CCW) to clockwise (CW) rotation. When peritrichous flagella of *E. coli* rotate CCW, the bacterial cell runs, whereas CW rotation results in tumbling, which serves to reorient the swimming direction. Although phosphorylated CheY (CheY-P) autodephosphorylates, a phosphatase known as CheZ in *E. coli* (or CheX/CheC in other bacteria/spirochetes) dephosphorylates the CheY-P, resulting in CW rotations. Thus, the levels of CheY-P determine whether a cell runs or tumbles (19–21).

The chemotaxis signaling system is conserved among prokaryotes (22). The *B. burgdorferi* genome possesses a sophisticated chemotaxis system with multiple motility- and chemotaxis-related operons (23, 24). Genomic sequencing as well as *in vitro* functional analyses indicate that *B. burgdorferi* encodes multiple copies of the chemotaxis genes, including two histidine kinases (CheA1 and CheA2), three response regulatory proteins (CheY1, CheY2, and CheY3), three coupling proteins (CheW1, CheW2, and CheW3), two sets of chemotaxis adaptation proteins, CheB (CheB1 and CheB2) and CheR (CheR1 andCheR2), five MCPs, and one cytoplasmic chemoreceptor (24–29). *B. burgdorferi* also possesses a CheX phosphatase which we recently reported generates enhanced activity via CheD (12, 30, 31). Moreover, all of the motility and chemotaxis operons of *B. burgdorferi* are transcribed by the σ^{70} promoter (23). While the roles of many of those chemotaxis genes have been evaluated *in vitro*, only three (*cheA2*, *cheD*, and *cheY3*) have currently been investigated in the natural infectious life cycle of *B. burgdorferi* (11–13).

B. burgdorferi is a long (10 to 20 μm) and thin (0.3 μm) organism that possesses 7 to 11 periplasmic flagella attached to each end of the cell (9, 32). Tracking *B. burgdorferi* motility reveals three different swim modes: run, flex, and reverse. Runs occur when the periplasmic flagellar motors at one end of the cell rotate in the opposite direction of the motors at the other end (CW rotation in motors at one end of the cell and CCW rotation in motors at the other end). Spirochetes flex when the motors at both ends rotate in the same direction, i.e., both rotating either CW or CCW. Cell reversal occurs in translating cells when the motors at each end reverse their direction of rotation. The spirochete flex is thought to be equivalent to the *E. coli* or *S*. Typhimurium tumble (21, 26, 31, 33, 34).

The three *B. burgdorferi cheY* genes are located in three separate operons. Using functional and phosphorylation analyses, we have previously reported that these response regulatory proteins are phosphorylated by both of the histidine kinases, CheA1 and CheA2 (25, 31). However, only *cheY3* was found to be essential for motility and chemotaxis *in vitro* (25). Specifically, while wild-type (WT) *B. burgdorferi* cells are observed to run, pause/flex, and then change their swimming direction, *cheY3* mutant (Δ*cheY3*) cells constantly run in one direction without reversing and are subsequently deficient in chemotaxis (25). Recently, *cheY3*-mediated chemotaxis was found to be crucial for motility *in vivo*, including dissemination and viability in mice and ticks (13). Moreover, the CheY proteins do not functionally overlap each other (25). Since *B. burgdorferi* survives primarily within the disparate environments of tick and mammalian hosts in nature, we assume that one or more *cheY* genes are required for viability in ticks and/or persistence in the murine host, and these different proteins may provide different functions within these hosts. CheY proteins were also reported to be impor-

tant for host tissue colonization by several species of pathogenic bacteria, such as *Helicobacter pylori* and *Vibrio cholerae* (35–39). For our current studies, we intend to delineate the importance of the CheY2 response regulator for dissemination and persistence within both their arthropod and murine hosts. Our findings suggest that CheY2 provides different functions within these two hosts compared to our previous observations with a Δ*cheY3* mutant, and we propose a model suggesting how CheY2 could operate in the Lyme disease spirochete.

RESULTS

Construction of two independent *cheY2* mutants. The *B. burgdorferi cheY2* gene is located at the end of an operon consisting of *cheW2-orf0566-cheA1-cheB2-orf0569-cheY2* genes (Fig. 1A) (26). This operon is transcribed by the σ^{70} subunit of RNA polymerase (25, 26). We have previously reported that *cheY2* was not essential for motility or chemotaxis *in vitro* (25). However, those mutants were constructed in a high-passage, noninfectious strain and cannot be evaluated for their role in the enzootic life cycle of *B. burgdorferi* (in mouse or tick-mouse models of Lyme disease) (25). To assess the role of *cheY2* in the *B. burgdorferi* pathogenic cycle, the gene was inactivated singly using a kanamycin or a streptomycin resistance cassette in two different wild-type clones, B31-A3 (A3) and B31-A3-K10 (K10), respectively. The two independent single mutants were confirmed by genotyping using PCR (data not shown) and immunoblotting using *B. burgdorferi* CheY2-specific polyclonal antiserum (Fig. 1B) (25).

Because the targeted *cheY2* gene is located at the end of the operon, a polar effect on downstream gene expression is unlikely. Moreover, using the same protocol, we have created a *cheY2* mutant in the high-passage-number avirulent strain that exhibits no phenotypic alterations (25). Additionally, to exclude the possibility of a secondary alteration elsewhere in the genome, we attempted to complement the mutants using

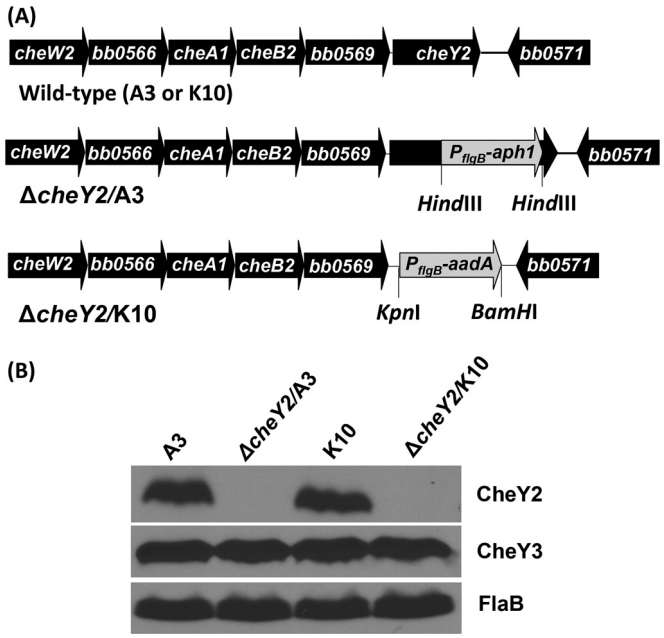

FIG 1 Inactivation and confirmation of two independent Δ*cheY2* mutants. (A) The *B. burgdorferi cheY2* operon consists of *cheW2*, *bb0566*, *cheA1*, *cheB2*, *bb0569*, and *cheY2* genes (diagram is not to scale). The *cheY2* gene was inactivated by inserting the P_{flgB}-*aph1* or P_{flgB}-*aadA* cassette using allelic exchange mutagenesis in the B31-A3 (A3) or B31-A3-K10 (K10) wild-type background, respectively. (B) Inactivation of the *cheY2* gene was confirmed by immunoblotting using whole-cell lysates from the indicated *B. burgdorferi* cells that were subjected to SDS-PAGE followed by probing with *B. burgdorferi* CheY2-specific polyclonal antisera. The antiserum reacted with the 10-kDa CheY2 protein in wild-type cells, as expected, and this protein is absent from the Δ*cheY2* mutants (both clones). FlaB and CheY3 were used as loading controls.

an intact *cheY2* gene, as described previously (6, 40). Even though our group has successfully generated numerous *B. burgdorferi* mutants in the past, our multiple attempts to complement the mutant in *cis* or in *trans* were unsuccessful, which is not uncommon due to the challenging nature of *B. burgdorferi* genetic manipulation. To best address this issue, we constructed two independent *cheY2* mutants instead of complementing the mutant, as others have done in the past (7, 41–45). Since a complemented strain was not constructed or analyzed, the observed phenotypes (discussed below) could result from a secondary mutation elsewhere in the genome. Importantly, both mutant cell types showed similar phenotypes, suggesting that the characteristics observed with the current *cheY2* mutants (Δ*cheY2*/A3 and Δ*cheY2*/K10) appear to be attributed to the *cheY2* mutation. Furthermore, linear and circular endogenous plasmids of the mutants were verified by PCR, and all clones retained the plasmids possessed by the parental wild-type cells (data not shown) (40, 46).

***In vitro* chemotaxis and motility phenotype of Δ*cheY2*/A3 and Δ*cheY2*/K10 mutants.** To determine if the two Δ*cheY2* strains exhibit any altered motility or chemotaxis phenotype, we assessed both the bacterial swimming rate and swarm plate chemotaxis assays, as described previously (25, 47, 48). Both Δ*cheY2* strains exhibit swimming patterns (run-pause/flex-reverse) and motility phenotypes that are indistinguishable from their respective wild-type parental cells (swimming velocity, 7.5 ± 1.1 μm/s versus 7.1 ± 0.9 μm/s by the wild-type clones; data not shown). Furthermore, swarm plate assays indicated that the chemotaxis phenotype of either Δ*cheY2* strain was not significantly altered compared to the parental wild-type cells (Fig. 2A). A modified swarm plate assay was also performed to more accurately assess the chemotactic behavior of individual bacteria (12, 13). The swarm plate assay is a group event where millions of bacteria attempt to migrate from the initial site of inoculation (in a semisolid plate) as they respond to chemotactic materials and metabolize neighboring nutrients, resulting in a swarm ring. However, results obtained from such an assay may not accurately determine the chemotactic ability of an individual spirochete. Accordingly, we plated 20 to 50 *B. burgdorferi* cells in a semisolid plate (the same plates as those used for the swarm plate assays) to determine the chemotactic ability of individual cells by measuring their colony swarm size. Prolonged incubation of those

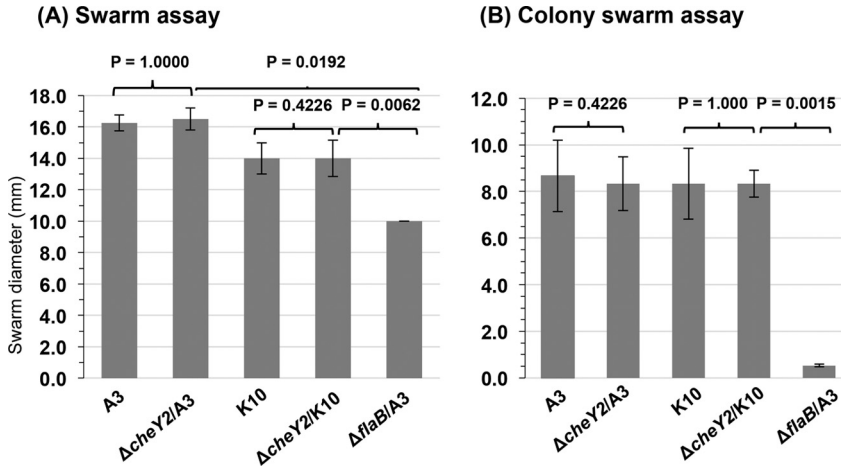

FIG 2 *B. burgdorferi* Δ*cheY2* mutants are not deficient in chemotaxis *in vitro*. (A) Swarm plate assays using 10^6 *B. burgdorferi* cells from the indicated strains were spotted onto 0.35% soft-agarose plates. Plates were incubated for 6 days, and the diameter of each clone was measured (in millimeters). A nonmotile Δ*flaB* mutant was used as a control (7). Bars represent means ± standard deviations from 3 independent plates. (B) *B. burgdorferi* wild-type and mutant cells were plated (10 to 50 cells per plate) separately in 0.35% soft agarose containing BSK growth medium that was diluted 10× with PBS and incubated for 4 weeks. Numbers are indicative of the means ± standard deviations of the means from at least 12 individual colonies (per clone per assay). Statistical analyses were performed using Student's paired *t* test to determine the *P* values between the wild type and mutants. A *P* value of <0.05 between strains was considered significant.

plates produced colony sizes that were not statistically different from those of the parental wild-type cells ($P = 0.38$ and $P = 0.27$, respectively) (Fig. 2B). Together, these data are the same as those reported previously, which suggest that a mutation in *cheY2* has little to no effect on motility or chemotaxis *in vitro* (25).

Δ*cheY2*/A3 and Δ*cheY2*/K10 mutants are severely attenuated in their abilities to persist or disseminate within C3H/HeN mice. To determine if the Δ*cheY2* strains are able to establish an infection in the mammalian host, we intradermally inoculated 5×10^6 *in vitro*-grown *B. burgdorferi* wild-type and Δ*cheY2* mutant bacteria in separate groups of mice ($n = 4$). Immediately before the injections, we verified by PCR that the endogenous *B. burgdorferi* plasmids are retained in the wild-type clones and their respective isogenic mutants (not shown). Four weeks postinoculation, the mice were euthanized and bacterial persistence was determined by the growth of the spirochetes from the isolated mouse tissues (ear skin, ankle joints, and urinary bladder) incubated in Barbour-Stoenner-Kelly II (BSK-II) growth medium. While the wild-type spirochetes were detected from all mouse tissues assessed, mutant *B. burgdorferi* (both clones) was detected in only a single bladder tissue out of 12 total tissue samples from four mice (Table 1). To validate the bacterial outgrowth analysis, DNA was isolated from each of those mouse tissues except the bladder tissue, followed by PCR to detect *B. burgdorferi flaB* DNA. Our PCR data indicate that DNAs from all of the mouse tissue samples were able to detect wild-type bacterial genomes (both clones), whereas none of the tissue samples were positive for the mutant genomes (both clones) (Table 1 and data not shown). These results suggest that CheY2 is crucial for establishing a disseminated infection in the murine host.

To better delineate whether the attenuated Δ*cheY2* strains are able to survive at the injection site skin tissue of the mice and/or disseminate from the skin to the distant tissues or whether the bacteria were efficiently cleared by the immune responses, groups of mice were inoculated with wild-type and mutant *B. burgdorferi* and subsequently euthanized at various times (24 h and 1 and 2 weeks postinjection). Tissue samples from each mouse were processed to recover live spirochetes from the culture as well as for bacterial genome quantification by quantitative PCR (qPCR). As shown in Table 2, the wild-type and Δ*cheY2* cells were reisolated from all injection site skin tissues when the mice were euthanized 24 h postinjection. When the mice were euthanized 1 week postinjection, wild-type cells were recovered from the injection site as well as from the distant tissues (ear or bladder), suggesting bacterial dissemination. Alternatively, Δ*cheY2* cells were not recovered from the injection site of any mouse tissues assessed at ≥1 week postinfection and were only recovered from a single distant ear skin tissue site out of 12 tissues processed from four mice (Table 2). Moreover, when the mice were euthanized 2 weeks postinjection, wild-type spirochetes were found to be disseminated to the distant tissues in all four mice. However, the mutant spirochetes were not able to be reisolated from any mouse tissues (Table 2).

To determine if mutant spirochetes were disseminated to the distant tissues but were unable to be accurately detected by regrowth assays and/or were cleared/reduced by the host immune responses, parallel mouse tissue samples were processed

TABLE 1 Δ*cheY2* spirochetes are severely attenuated in murine infection via regrowth analyses[a]

B. burgdorferi clone	Dose per mouse	No. of mouse tissues colonized/no. analyzed	No. of mice infected/no. analyzed
WT (A3)	5×10^6	11/12	4/4
Δ*cheY2*/A3	5×10^6	01/12	1/4[b]
WT (K10)	5×10^6	10/12	4/4
Δ*cheY2*/K10	5×10^6	01/12	1/4[b]

[a]C3H/HeN mice were injected intradermally/subcutaneously using the indicated *in vitro*-grown spirochete clones. Mice were euthanized 4 weeks post injection, and infectivity was determined by reisolation of *B. burgdorferi* from the tissue samples (ear, joint, and bladder from each mouse). Doses shown are the actual numbers of spirochetes injected in each mouse.

[b]Δ*cheY2*/A3 or Δ*cheY2*/K10 mutant was detected in only one bladder tissue of a mouse.

TABLE 2 *B. burgdorferi* Δ*cheY2* mutant is attenuated for persistent infection and dissemination within mice via regrowth analyses[a]

B. burgdorferi clone and euthanization time postinjection	No. cultures positive/no. tested				No. of mice infected/ no. tested
	Injection site skin	Distant skin	Bladder	Joint	
WT (A3)					
24 h	4/4	0/4	0/4	0/4	4/4
1 week	2/4	2/4	1/4	0/4	3/4
2 week	0/4	4/4	4/4	4/4	4/4
Δ*cheY2*/A3					
24 h	3/4[b]	0/4	0/4	0/4	3/4
1 week	1/4	0/4	0/4	0/4	1/4
2 week	0/4	0/4	0/4	0/4	0/4

[a]C3H/HeN mice were injected intradermally/subcutaneously (into ear skin for 24 h postinjection or dorsal skin for 1 to 2 weeks postinjection) using the indicated *in vitro*-grown spirochete clones. Approximately 5×10^6 spirochetes were inoculated per mouse as verified by CFU. Mice were euthanized at the indicated time points, and infectivity was determined by reisolation of *B. burgdorferi* from the tissue samples.
[b]An injection site skin tissue could have been processed mistakenly.

for DNA isolation followed by *B. burgdorferi* genome quantitation using qPCR (Fig. 3). At 24 h postinjection, the numbers of Δ*cheY2* genomes in the skin injection site were more than those detected for wild-type bacteria, suggesting that our inoculum of Δ*cheY2* mutant was actually greater than that of wild-type bacteria. However, by 1 week postinjection the numbers of Δ*cheY2* genomes at the injection site were significantly reduced compared to the original inoculum at 24 h and were over 100-fold less than those of the wild-type bacterial genomes at 1 week postinjection at the inoculation site ($P = 0.006$), suggesting that only wild-type *B. burgdorferi* multiplied. Additionally, wild-type bacteria were detected at distant skin sites at 1 week postinjection, whereas no Δ*cheY2* genomes were detected at the distant site at this time, again suggesting that this mutant is unable to efficiently disseminate from the inoculation site (Fig. 3). Finally, at 2 weeks postinjection, Δ*cheY2* genomes were barely detected in the skin injection

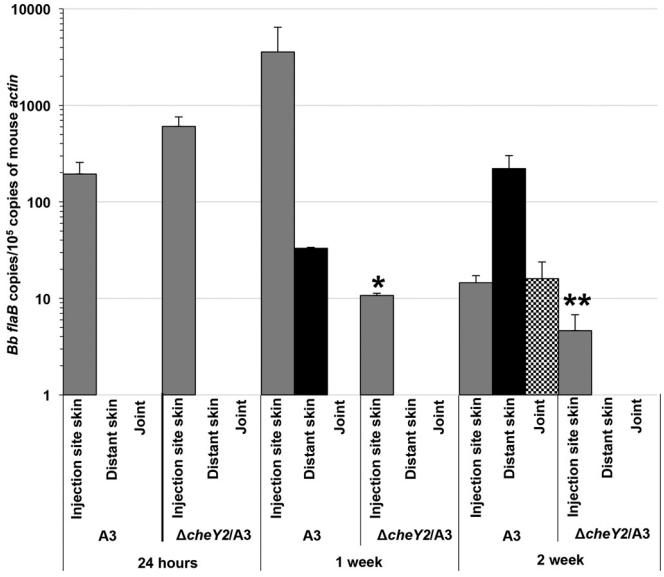

FIG 3 Relative number of *B. burgdorferi* genomes in mouse tissues as determined by qPCR. Groups of C3H/HeN mice ($n = 4$ per clone per time point) were injected with 5×10^6 wild-type or Δ*cheY2* mutant bacteria via the intradermal dorsal or ear skin route (24 h). Mice were euthanized at the indicated time points. Mouse tissues were processed for DNA purification followed by qPCR. The number of *B. burgdorferi flaB* copies was normalized to the number of mouse *β-actin* copies. Each bar represents means of data from four mouse tissues ± standard deviations of the means. *Bb*, *B. burgdorferi*. *, $P < 0.006$; **, $P < 0.01$. A bar is not shown for some tissues because bacterial genome was not detected.

site and were never detected in any distant tissue assessed, whereas wild-type genomes were detected in both the local inoculation site and all distant tissues assessed (Fig. 3). Overall, these qPCR data match fairly well with the bacterial reisolation shown in Table 2, although the qPCR appears to be more sensitive in detecting the Δ*cheY2* bacteria, potentially due to a decreased ability of these mutants to migrate out of the collected tissues for the tube-based regrowth assays. Importantly, these data suggest that the Δ*cheY2* bacteria are attenuated both in their ability to establish a persistent infection at the skin inoculation site as well as their ability to disseminate to distant target tissues and/or evade immune clearance at those sites.

Δ*cheY2* mutant spirochetes are unable to infect mice by tick bite. The *B. burgdorferi* natural enzootic cycle requires that the bacteria establish persistent infection within both tick and vertebrate hosts. Because the Δ*cheY2* mutants were severely attenuated in mice by needle inoculation, it is impractical to assess their ability to infect naive ticks by natural acquisition (i.e., via feeding on infected mice, followed by determination of spirochete transmission [tick to mouse]) (6, 7, 48). To address the possibility that the Δ*cheY2* strain can establish infection in naive mice via tick bite, *Ixodes scapularis* nymphs were artificially infected by immersion with either the wild type or isogenic Δ*cheY2* mutants before being encapsulated and allowed to feed on naive C3H/HeN mice (15 nymphs per mouse, 3 mice per strain per assay). Seven days after ticks dropped off the mice, ticks were surface sterilized and then squashed individually to isolate genomic DNA to determine spirochete densities using enolase gene-specific qPCR, as described previously (Fig. 4) (6). The Δ*cheY2* strain displayed densities similar to those of wild-type bacteria in ticks both before (i.e., unfed) and after (i.e., fed) feeding on mice ($P = 0.19$ and $P = 0.26$, respectively, in unfed ticks; $P = 0.17$ and $P = 0.65$, respectively, in fed ticks), suggesting they persist within fed and unfed ticks similar to wild-type bacteria. To determine if infected ticks transmit the Δ*cheY2* spirochetes in mice and establish persistent infection, mouse tissues were collected either 48 h or 2 weeks after tick repletion. Bacterial reisolation from both the tick-feeding site and distant tissues indicate that no assessed tissues were positive for the Δ*cheY2* strain, whereas all tissues from mice fed on by the wild-type infected nymphs demonstrated bacterial growth (Table 3). qPCR analyses performed on mouse tissues from parallel studies produced results similar to those of the regrowth studies (not shown). Together, these results suggest that Δ*cheY2* mutants are not able to establish an infection in mice via tick bite, even though the mutants survived normally in nymphal ticks. Finally, these studies observed no differences between

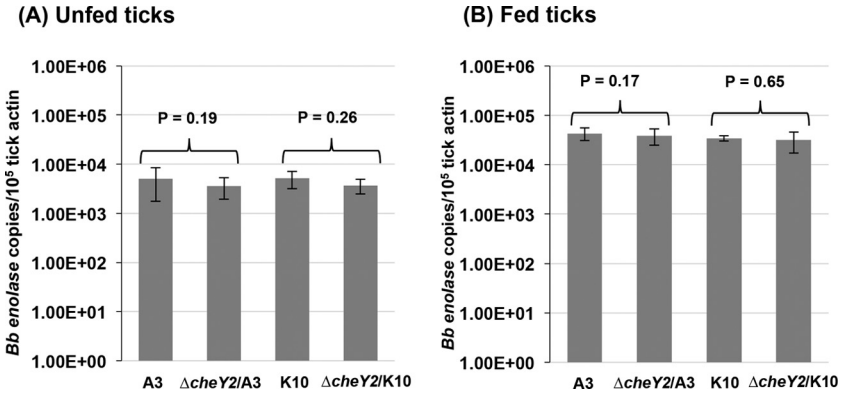

FIG 4 Viability of Δ*cheY2* mutants in unfed and fed nymphs. Naive nymphs were artificially infected as described in Materials and Methods. A subset of immersed nymphs was allowed to feed on separate naive C3H/HeN mice. Seven days after feeding, fed (B) and unfed (A) ticks were processed for PCR analysis to determine spirochete-positive ticks, and subsequently qPCR was performed to determine the number of spirochete genomes using enolase gene-specific primers. Results shown are means ± standard deviations of the means from at least five spirochete-positive ticks per clone per assay. Representative data from two independent studies are shown here. A *P* value of <0.05 between strains is considered significant.

TABLE 3 Δ*cheY2* spirochetes were not able to infect naive C3H/HeN mice by tick bite[a]

Nymphs infected with *B. burgdorferi* clone	No. of mice infected by tick bite/no. challenged
WT (A3)	5/6
Δ*cheY2*/A3	0/6
WT (K10)	5/6
Δ*cheY2*/K10	0/6

[a]Nymphal ticks were infected with the indicated *B. burgdorferi* strains by immersion in liquid cultures and were subsequently allowed to feed on naive mice. Fifteen infected encapsulated nymphs per mouse were allowed to feed to repletion. Two weeks (or 48 h; data not shown) after feeding, mice were euthanized to determine bacterial growth from the tissues.

mutants generated on both genetic clones (Δ*cheY2*/A3 and Δ*cheY2*/K10) in all *in vitro* or *in vivo* assays.

DISCUSSION

Chemotaxis signal transduction systems typically govern the rotation of flagellar motors, which allows a bacterium to respond and survive in a challenging environment. Even though more than 50% of all sequenced prokaryotic genomes contain at least one chemotaxis system, many of those genomes possess multiple sets of chemotaxis genes, and at least one of them is dedicated to controlling motility (22, 49–51). In most bacterial species that possess multiple sets of chemotaxis genes, very little is known about what role these additional chemotaxis genes perform. However, there are a few instances in which multiple chemotaxis-like signaling systems appear to have very different roles in the same species. For example, *Myxococcus xanthus* possesses eight sets of chemotaxis-like genes. Three of them control the frequency of gliding motility reversals, exopolysaccharide (EPS) synthesis, and entry into the myxospore developmental pathway (52–54). These and other recent reports suggest that some chemotaxis-like signaling pathways control other cellular nonchemotactic processes. However, in each of those cases it is not clear whether the effect on transcription is direct or indirect or if those chemotaxis-like proteins possess a DNA binding domain (52, 54–58). Importantly, most typical CheY chemotaxis response regulatory proteins lack the DNA-binding domain; thus, these proteins generally do not modulate gene expression. These CheY proteins instead bind to a flagellar protein (FliM/FliN) to alter cellular swimming behavior (22, 59, 60). Based on this model, similar *cheY2* mutant cells would be expected to exhibit altered motility and deficient chemotaxis phenotypes similar to that observed in many bacterial *cheY* mutants, including the *B. burgdorferi cheY3* mutants (13, 25, 50, 56). However, the *cheY2* mutants produced in our study exhibited *in vitro* motility and chemotaxis phenotypes that are indistinguishable from the wild-type parental spirochetes (Fig. 2). This lack of an altered motility/chemotaxis phenotype is not without precedent. The *Vibrio cholerae* genome was reported to possess five CheY proteins, and only two of them (CheY3 and CheY4) are required for motility/chemotaxis *in vitro*; the functions of the other CheY proteins are unknown (36, 51). Previously, any *cheY* mutant that was observed to exhibit an altered motility/chemotaxis phenotype was also found to have deficiencies in virulence; examples include a *B. burgdorferi cheY3* mutant and *V. cholerae cheY3* and *cheY4* mutants (13, 35, 36, 51). Conversely, when a *cheY* mutation does not alter the motility/chemotaxis phenotype *in vitro*, those *cheY* mutants exhibit wild-type abilities in colonizing animal hosts (35, 36, 51). Surprisingly, our observations with *B. burgdorferi cheY2* mutants appear to be an exception, as these Δ*cheY2* cells appeared normal *in vitro* but were significantly attenuated in murine infection (Tables 1 and 2 and Fig. 3).

Interestingly, nymphal ticks colonized with Δ*cheY2* bacteria were not able to establish persistent infection in naive mice, even though the densities of mutant spirochetes were similar to wild-type levels in both fed and unfed ticks that were infected by immersion, suggesting that the CheY2 defect was only apparent either during the transmission from the tick host into mouse tissues and/or when these bacteria were within murine host tissues (Table 3 and Fig. 4). This persistence phenotype within the

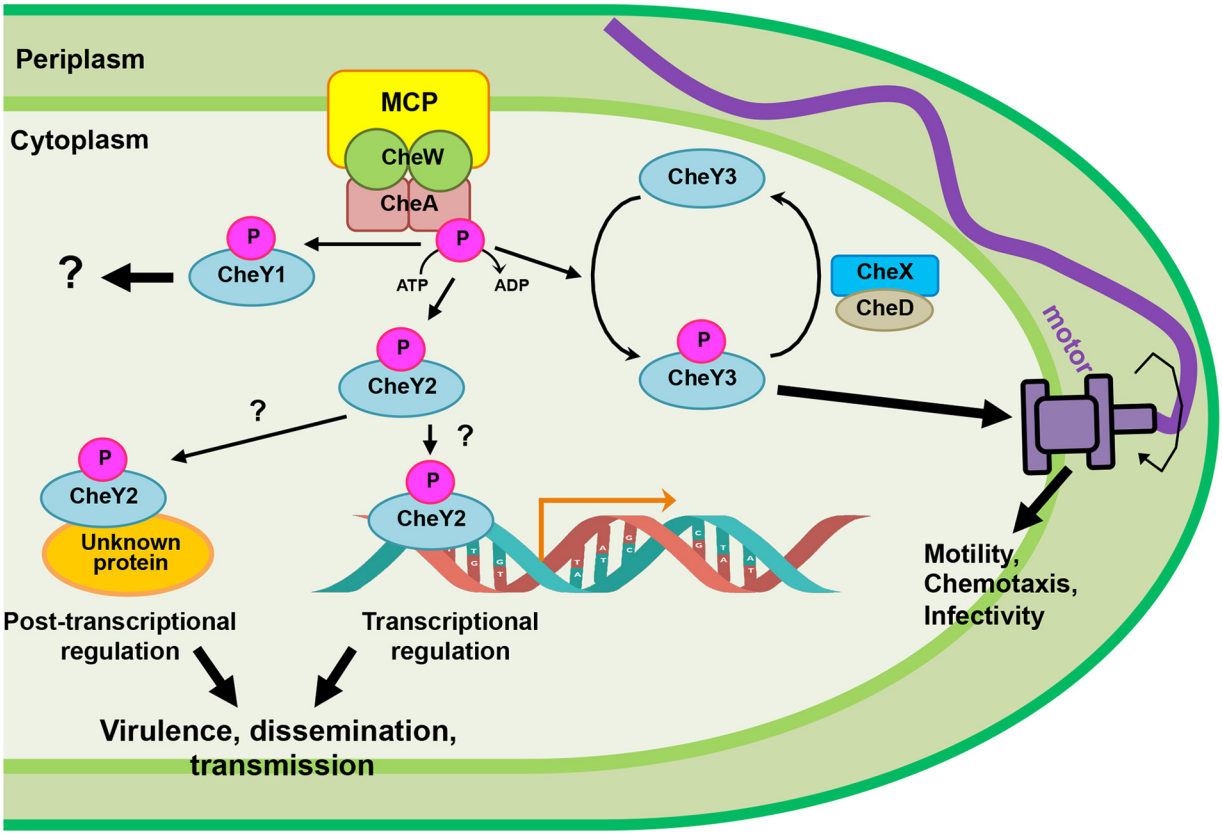

FIG 5 Working model of CheY2 functions in *B. burgdorferi* enzootic cycle. A simplistic chemotaxis signaling pathway of *B. burgdorferi* is depicted. Based on our findings, we propose that after phosphorylation by the histidine kinase CheA, CheY3-P binds to the flagellar switch proteins to alter bacterial swimming behavior. Consequently, *cheY3*-mediated chemotaxis is found to affect dissemination and viability of *B. burgdorferi* in mice and ticks (13). Dephosphorylation of CheY3-P is mediated by CheX-CheD (12). Our current data suggest that CheY2 does not affect motility or chemotaxis despite having all domains/conserved amino acid residues seen in a classical CheY protein (25). Because the mice are not being infected or partially infected by needle inoculation or tick bite, we propose that CheY2, after being phosphorylated by CheA, acts as a virulence determinant in *B. burgdorferi*. Instead of controlling motility, this CheY2-P may act as a transcriptional or posttranscriptional regulator to modulate *B. burgdorferi* gene expression or a protein's function/activity. Alternatively, its elevated expression in fed ticks may alter the bacterial or host gene functions in order for the spirochete to transmit from the vector to the murine host. The function of *cheY1* in the enzootic cycle is unknown. As described in the text, *B. burgdorferi* possesses five MCPs, three CheW and two CheA proteins.

tick is different from that recently observed by a nonmotile Δ*motB* strain possessing an intact chemotaxis system, in that the Δ*motB* bacteria maintained wild-type numbers in the unfed tick but were rapidly reduced in the tick after taking a blood meal (6). It was speculated that the nonmotile Δ*motB* bacteria were unable to generate certain interactions within the tick environment that allows protection against bactericidal factors present in the ingested blood meal (10). Similarly, a Δ*cheY3* spirochete that could achieve normal swimming speeds but was unable to reverse directions both *in vitro* and *in vivo* was also shown to possess normal numbers in unfed ticks, but the numbers were reduced in fed ticks (13). *B. burgdorferi cheY2* expression is reported to be elevated in fed ticks compared to a mammalian-host adapted condition, indicating this pathway is active subsequent to tick feeding (61). Thus, the chemotaxis/motility properties guided by CheY2 should be sufficient to allow wild-type spirochetes to either migrate to a desired environment within the tick and/or to resist clearance by immune mediators present within the blood materials acquired during feeding. This is also supported by studies demonstrating that even *B. burgdorferi* strains with limited motility can survive efficiently in fed ticks (our unpublished observations). This finding for host-specific motility/chemotaxis deficiencies is unprecedented, and this paradigm may provide a model system for better understanding the unique virulence mechanisms required to persist within vertebrate versus arthropod hosts.

It is currently unclear as to why Δ*cheY2* spirochetes show defects in their abilities

to disseminate and establish infection in mouse tissues either by tick bite or needle inoculation. Since Δ*cheY2* bacteria demonstrate normal motility/chemotaxis *in vitro*, they appear to be capable of traversing the tight junctions of the tick midgut epithelial cells that is required for transmission of *B. burgdorferi* from the tick midgut into murine skin, making it less likely that the deficiencies observed in murine infections were due to a defect in transmission, although this is certainly possible. *B. burgdorferi cheY2* expression is elevated in fed ticks despite the fact that the operon is transcribed by the σ^{70} promoter, suggesting this pathway is active subsequent to feeding (61). These findings also suggest that CheY2 possesses some function(s) that is atypical for a chemotaxis response regulator, even though this response regulatory protein contains all of the conserved amino acid residues of CheY and is being phosphorylated by the histidine kinases (25, 26). This would not be unprecedented, as chemotaxis-like signaling systems have been described to perform nonchemotactic cellular functions in several species of bacteria (52–56). We could surmise that CheY2 performs a role other than that of the typical chemotaxis signaling system (Fig. 5), such as binding to an operon promoter or a protein to modulate some virulence determinants in *B. burgdorferi* (e.g., CheY exerts transcriptional or posttranscriptional regulation). Consequently, a mutation in *cheY2* would mediate altered expression of those putative virulence-associated genes, resulting in attenuated mouse infection or dissemination (Fig. 5). Alternatively, since *B. burgdorferi* is found only within vertebrate or tick hosts during their natural enzootic cycles, the *in vitro* assay systems used to observe motility/chemotaxis phenotypes likely do not accurately reflect the *in vivo* environment in either ticks or vertebrate hosts. As such, we realize that the *cheY2* mutant may exhibit the altered motility/chemotaxis phenotype only within its native hosts. Ideally, generation of a fluorescently labeled Δ*cheY2* clone will allow us to delineate any apparent defects within murine tissues using our intravital microscopy models, as we recently reported for the Δ*motB* and Δ*cheY3* mutants (6, 13). Regardless, a more detailed analysis of these CheY2-mediated signaling pathways will be required to unravel the complex regulation this distinctive organism performs during its enzootic infection cycle.

MATERIALS AND METHODS

Ethics statement. East Carolina University is accredited by the International Association for Assessment and Accreditation of Laboratory Animal Care. Protocols for tick and animal experimentations were approved by the East Carolina University Animal Care and Use Committee.

Bacterial strains and growth conditions. Low-passage, virulent *B. burgdorferi* strains B31-A3 and B31-A3-K10 (a kind gift from R. Rego and P. Rosa, Rocky Mountain Laboratories, NIH) were used as wild-type (WT) clones in this study (62, 63). B31-A3-K10 is a derivative of B31-A3 in which the *bbe002* gene located in linear plasmid 25 (lp25) was inactivated using a P_{flaB}-*aph1* (Kan^r) cassette to increase transformation frequency (63). The genome of the parent strain B31 is known to contain 12 linear and 9 circular plasmids, for a total of 21 plasmids, in addition to a 960-kbp linear chromosome (24, 64). The WT clones used in this study retain all endogenous plasmids except circular plasmid 9 (cp9). Construction of the *cheY2* mutants in *B. burgdorferi* strains B31-A3 (referred to as A3) and B31-A3-K10 (K10) are described below. *B. burgdorferi* cells were grown in liquid Barbour-Stoenner-Kelly II (BSK-II) medium, and cells were plated using plating BSK (P-BSK), which was prepared using 0.5% agarose. Cells were grown at 35°C in a 2.5% CO_2 incubator as previously described (65). *Escherichia coli* strains were cultivated in Luria-Bertani broth (1% tryptone, 1% NaCl, 0.5% yeast extract). When required, culture and plating medium were supplemented with appropriate antibiotics at the following concentrations: 200 μg/ml kanamycin, 100 μg/ml streptomycin or spectinomycin, or 100 μg/ml ampicillin.

Construction of *cheY2* mutants. Construction of the *cheY2* inactivation plasmids, electroporation, and plating conditions were described previously (7, 8). To construct a *cheY2* mutant in the B31-A3 background, the *cheY2* gene (gene locus number *bb0570*) and flanking DNA was first amplified by PCR from the chromosomal DNA of *B. burgdorferi* strain B31-A3 using primers CheY2-KO-F (TCTGCTAGGTTT CAAAATAT) and CheY2-KO-R (TGGACTTACCCT TTACATAG), and the product obtained was cloned into plasmid pGEM-T Easy (Promega Inc.). The *cheY2* gene was inactivated using a kanamycin resistance cassette (P_{flgB}-*aph1*), which was inserted at the HindIII sites located within *cheY2* (66). DNA containing *cheY2*-P_{flgB}-*aph1* was linearized by restriction digestion to remove the ampicillin marker of the vector and electroporated into competent B31-A3 cells to obtain mutants. Kanamycin-resistant transformants were screened by PCR for proper recombination of the *cheY2* inactivation cassette in the genome. Western blot analysis was used to confirm the inactivation of *cheY2* using *B. burgdorferi* CheY2-specific antisera as described below (25).

To construct the *cheY2* mutant in B31-A3-K10, the 5′ (968 bp)- and 3′ (919 bp)-flanking regions of the *cheY2* gene were amplified by PCR from chromosomal DNA of *B. burgdorferi* strain B31-A3-K10 using primers CheY2mut-F (CGGATACATCAAAAGTTATAGTAAAAGATG) and CheY2mut.KpnI-R (GGT ACCTAATTTTCTCCTAAAACCCT) as well as CheY2mut.BamHI-F (GGATCCGTTTATATTTGCAATTAATT TGT) and CheY2mut-R (GGTGGAGGAAGAGTTGCAAG). A spectinomycin-streptomycin resistance cassette fused with *B. burgdorferi flgB* promoter (P_{flgB}-*aadA*) was similarly PCR amplified from a pKFSS1 shuttle vector using primers P_{flgB}Strep.KpnI-F (GGTACCTACCCGAGCTTCA) and P_{flgB}Strep.BamHI-R (GGATCCAAGCTTGACGTCATTA) (67). These three pieces of DNA fragments were individually cloned into plasmid pGEM-T Easy (Promega Inc.). The pieces were cloned together using restriction digestion. First, the 5′-flanking regions of *cheY2* and P_{flgB}-*aadA* were cloned together using KpnI and SacI restriction digestion, yielding plasmid Teasy::5′Y2-P_{flgB}-*aadA*. The 3′-flaking region of the *cheY2* fragment then was cloned into Teasy::5′-cheY2-P_{flgB}-*aadA* using BamHI and SacI restriction digestion, yielding plasmid Teasy::cheY2_KO-P_{flgB}-*aadA*. Competent B31-A3-K10 cells were electroporated with cheY2_KO_P_{flgB}-*aadA* DNA as described above (8, 65). The transformants were selected with streptomycin. The streptomycin-resistant transformants were confirmed by PCR and Western blotting as described above.

SDS-PAGE and Western blot analysis. SDS-PAGE and immunoblotting with an enhanced chemiluminescent detection method were carried out as reported previously (GE Health Inc.) (6). Protein concentrations of cell lysates were determined with a Bio-Rad protein assay kit using bovine serum albumin as a standard. A volume of cell lysate equivalent to 10 μg of protein was subjected to SDS-PAGE and immunoblotting using *B. burgdorferi* CheY2-, CheY3-, and FlaB-specific antibodies (25).

Microscopy and computer-assisted motion analysis. Live *B. burgdorferi* cells were observed under a Zeiss Axio Imager M1 dark-field microscope connected to an AxioCam digital camera. Exponentially growing cells (2×10^7 to 3×10^7 cells/ml) were mixed with 0.5% 400-mesh methylcellulose (Sigma-Aldrich Co.) and video recorded at room temperature (23°C). Cell swimming behavior and velocity were determined using AxioVision software (47). Results are expressed as velocity (mean distance, in micrometers, traveled by a given strain per second). At least 10 cells from each strain were analyzed (25, 47).

Chemotaxis assays. Swarm plate chemotaxis assays were performed using our established protocol described previously (65). Approximately 10^6 cells in a 5-μl volume were spotted onto a 0.35% agarose plate containing plating BSK medium diluted 1:10 in Dulbecco's phosphate-buffered saline. Since *B. burgdorferi* is a slow-growing organism (8- to 12-h generation time), plates were incubated for 6 days at 35°C in a 2.5% CO_2 humidified incubator (6, 7). At least three independent assays were performed. The chemotactic swarming ability of individual bacterial colonies of each strain was determined by plating no more than 50 cells into a 95-mm by 15-mm petri dish containing semisolid P-BSK diluted as described above (12, 13). Plates were incubated for 4 weeks, at which time colony diameters were measured. At least 12 colony diameters were measured for each strain in each assay. The paired Student *t* test was used to compare wild-type and mutant cell swarm diameters.

Mouse infection studies using needle-injected *B. burgdorferi*. Six- to seven-week-old C3H/HeN mice (Charles River Laboratories) were used for infection studies as previously described (41, 48, 68–70). In order to determine the infectious ability of the spirochetes, separate groups of mice were injected intradermally/subcutaneously in ear or dorsal/back skin tissue with *in vitro*-grown WT A3, WT K10, Δ*cheY2/A3*, or Δ*cheY2/K10* strain at the indicated doses. Spirochetal numbers were determined using a Petroff-Hausser chamber and verified via CFU by plating. Mice were euthanized 24 h, 1 week, 2 weeks, or 4 weeks after injection, and then multiple tissues were harvested aseptically from each mouse. The injection site skin tissue was cut into two equal portions. One part of the skin, as well as a joint, and ear tissue from each mouse ($n = 4$) were processed for DNA isolation followed by qPCR to determine bacterial density using *B. burgdorferi flaB* gene-specific primers (6, 7, 40). DNA levels were assessed by amplification of the *actin* gene for the mouse and *flaB* gene for *B. burgdorferi*. Copy numbers for mouse and *B. burgdorferi* genomes were evaluated by extrapolating to standard curves devised by Bio-Rad CFX Manager 3.1. Final *B. burgdorferi* numbers were calculated by normalizing *B. burgdorferi* genomes to 10^5 mouse genomes. The results are expressed as means $\pm$ standard deviations from four tissues collected from four mice. Statistical analyses were performed using Student's paired *t* test to calculate the significance of the normalized values between wild-type and mutant samples. A *P* value of 0.05 between samples was considered significant. The other half of the injection site skin, the second joint tissue, and the bladder from each mouse were placed in BSK-II broth for up to 35 days to allow bacterial growth, which is the direct determination of the ability of spirochetes to infect mice and disseminate throughout the body. The presence of spirochetes in the growth medium was determined by dark-field microscopy and is referred to as regrowth, outgrowth, or reisolation.

Assessment of spirochete transmission to mice by encapsulated nymphs. Transmission of spirochetes from *Ixodes scapularis* ticks to C3H/HeN mice was assessed using artificially infected nymphs as described previously (6, 48). Naive nymphal ticks were experimentally infected by immersion with exponential-phase (2 to 3×10^7 cells/ml) *B. burgdorferi* clones, and then we washed the immersed ticks with sterile distilled H_2O to remove the surface-attached spirochetes. The ticks were then kept in a humidified chamber for approximately 24 h before allowing them to feed on naive mice (7, 48, 71). Mice were anesthetized, and 15 nymphs were confined to a capsule affixed to the shaved back of a naive C3H/HeN mouse ($n = 3$ per strain per assay). The ticks were allowed to feed to repletion (3 to 5 days) and then collected from the capsules (6, 72). Fed and unfed (immersed) ticks were surface sterilized using 3% H_2O_2 and 70% ethanol, individually crushed on day 7 postrepletion to isolate genomic DNA using a DNeasy blood and tissue kit according to the manufacturer's instructions (Qiagen Inc.). The DNA from each tick was utilized for PCR to determine spirochete-positive ticks using *B. burgdorferi flaB* gene-specific

primers. Subsequently, each sample of spirochete-positive tick ($n = 5$) DNA was used to determine bacterial densities by qPCR using *B. burgdorferi* enolase gene-specific primers as described previously (40, 73, 74). Numbers of the copies of the *B. burgdorferi* enolase gene per tick were extrapolated from a standard curve generated using a known amount of plasmid DNA containing the enolase gene as the template and normalized to the tick *actin* gene. The results are expressed as means ± standard deviations from at least 5 sets of spirochete-positive tick data per clone per assay. Statistical analyses were performed using Student's paired *t* test to calculate the significance of the normalized values between wild-type and mutant samples. A *P* value of 0.05 between samples was considered significant.

Tick-fed mice were euthanized at 48 h or 2 weeks postrepletion. A section of skin comprising the tick-feeding site was excised, rinsed in 70% isopropanol, and cut into equal portions. Parts of the tick-bite site skin, ear, bladder, and joint tissues were cultured separately in BSK-II medium for up to 35 days to determine bacterial outgrowth, and the remaining tissues were processed for PCR to detect *B. burgdorferi* DNA using enolase gene-specific primers (6, 7, 40).

ACKNOWLEDGMENTS

We thank P. Rosa and R. Rego for sharing reagents and E. Novak for help.

This research was supported by grants from the National Institute of Allergy and Infectious Diseases (1R21AI113014) and the National Institute of Arthritis and Musculoskeletal and Skin Diseases (1R01AR060834).

REFERENCES

1. Mead PS. 2015. Epidemiology of Lyme disease. Infect Dis Clin North Am 29:187–210. https://doi.org/10.1016/j.idc.2015.02.010.
2. Kuehn BM. 2013. CDC estimates 300,000 US cases of Lyme disease annually. JAMA 310:1110. https://doi.org/10.1001/jama.2013.278331.
3. Groshong AM, Blevins JS. 2014. Insights into the biology of Borrelia burgdorferi gained through the application of molecular genetics. Adv Appl Microbiol 86:41–143. https://doi.org/10.1016/B978-0-12-800262-9.00002-0.
4. Radolf JD, Caimano MJ, Stevenson B, Hu LT. 2012. Of ticks, mice and men: understanding the dual-host lifestyle of Lyme disease spirochaetes. Nat Rev Microbiol 10:87–99.
5. Brisson D, Drecktrah D, Eggers CH, Samuels DS. 2012. Genetics of Borrelia burgdorferi. Annu Rev Genetics 416:513–534.
6. Sultan SZ, Sekar P, Zhao X, Manne A, Liu J, Wooten RM, Motaleb MA. 2015. Motor rotation is essential for the formation of the periplasmic flagellar ribbon, cellular morphology, and Borrelia burgdorferi persistence within Ixodes scapularis tick and murine hosts. Infect Immun 83:1765–1777. https://doi.org/10.1128/IAI.03097-14.
7. Sultan SZ, Manne A, Stewart PE, Bestor A, Rosa PA, Charon NW, Motaleb MA. 2013. Motility is crucial for the infectious life cycle of Borrelia burgdorferi. Infect Immun 81:2012–2021. https://doi.org/10.1128/IAI.01228-12.
8. Motaleb MA, Corum L, Bono JL, Elias AF, Rosa P, Samuels DS, Charon NW. 2000. Borrelia burgdorferi periplasmic flagella have both skeletal and motility functions. Proc Natl Acad Sci U S A 97:10899–10904. https://doi.org/10.1073/pnas.200221797.
9. Kudryashev M, Cyrklaff M, Baumeister W, Simon MM, Wallich R, Frischknecht F. 2009. Comparative cryo-electron tomography of pathogenic Lyme disease spirochetes. Mol Microbiol 71:1415–1434. https://doi.org/10.1111/j.1365-2958.2009.06613.x.
10. Motaleb MA, Liu J, Wooten RM. 2015. Spirochetal motility and chemotaxis in the natural enzootic cycle and development of Lyme disease. Curr Opin Microbiol 28:106–113. https://doi.org/10.1016/j.mib.2015.09.006.
11. Sze CW, Zhang K, Kariu T, Pal U, Li C. 2012. Borrelia burgdorferi needs chemotaxis to establish infection in mammals and to accomplish its enzootic cycle. Infect Immun 80:2485–2492. https://doi.org/10.1128/IAI.00145-12.
12. Moon KH, Hobbs G, Motaleb MA. 2016. Borrelia burgdorferi CheD promotes various functions in chemotaxis and pathogenic life cycle of the spirochete. Infect Immun 84:1743–1752. https://doi.org/10.1128/IAI.01347-15.
13. Novak EA, Sekar P, Xu H, Moon KH, Manne A, Wooten RM, Motaleb MA. 20 May 2016. The Borrelia burgdorferi CheY3 response regulator is essential for chemotaxis and completion of its natural infection cycle. Cell Microbiol https://doi.org/10.1111/cmi.12617.
14. Sourjik V, Wingreen NS. 2012. Responding to chemical gradients: bacterial chemotaxis. Curr Opin Cell Biol 24:262–268. https://doi.org/10.1016/j.ceb.2011.11.008.
15. Porter SL, Wadhams GH, Armitage JP. 2011. Signal processing in complex chemotaxis pathways. Nat Rev Microbiol 9:153–165. https://doi.org/10.1038/nrmicro2505.
16. Wadhams GH, Armitage JP. 2004. Making sense of it all: bacterial chemotaxis. Nat Rev Mol Cell Biol 5:1024–1037. https://doi.org/10.1038/nrm1524.
17. Falke JJ, Bass RB, Butler SL, Chervitz SA, Danielson MA. 1997. The two-component signaling pathway of bacterial chemotaxis: a molecular view of signal transduction by receptors, kinases, and adaptation enzymes. Annu Rev Cell Dev Biol 13:457–512. https://doi.org/10.1146/annurev.cellbio.13.1.457.
18. Sarkar MK, Paul K, Blair D. 2010. Chemotaxis signaling protein CheY binds to the rotor protein FliN to control the direction of flagellar rotation in Escherichia coli. Proc Natl Acad Sci U S A 107:9370–9375. https://doi.org/10.1073/pnas.1000935107.
19. Silversmith RE, Guanga GP, Betts L, Chu C, Zhao R, Bourret RB. 2003. CheZ-mediated dephosphorylation of the Escherichia coli chemotaxis response regulator CheY: role for CheY glutamate 89. J Bacteriol 185:1495–1502. https://doi.org/10.1128/JB.185.5.1495-1502.2003.
20. Zhao R, Collins EJ, Bourret RB, Silversmith RE. 2002. Structure and catalytic mechanism of the E. coli chemotaxis phosphatase CheZ. Nat Struct Biol 9:570–575.
21. Boesch KC, Silversmith RE, Bourret RB. 2000. Isolation and characterization of nonchemotactic CheZ mutants of Escherichia coli. J Bacteriol 182:3544–3552. https://doi.org/10.1128/JB.182.12.3544-3552.2000.
22. Wuichet K, Zhulin IB. 2010. Origins and diversification of a complex signal transduction system in prokaryotes. Sci Signal 3:ra50.
23. Charon NW, Cockburn A, Li C, Liu J, Miller KA, Miller MR, Motaleb MA, Wolgemuth CW. 2012. The unique paradigm of spirochete motility and chemotaxis. Annu Rev Microbiol 66:349–370. https://doi.org/10.1146/annurev-micro-092611-150145.
24. Fraser CM, Casjens S, Huang WM, Sutton GG, Clayton R, Lathigra R, White O, Ketchum KA, Dodson R, Hickey EK, Gwinn M, Dougherty B, Tomb JF, Fleischmann RD, Richardson D, Peterson J, Kerlavage AR, Quackenbush J, Salzberg S, Hanson M, van Vugt R, Palmer N, Adams MD, Gocayne J. 1997. Genomic sequence of a Lyme disease spirochaete, Borrelia burgdorferi. Nature 390:580–586. https://doi.org/10.1038/37551.
25. Motaleb MA, Sultan SZ, Miller MR, Li C, Charon NW. 2011. CheY3 of Borrelia burgdorferi is the key response regulator essential for chemotaxis and forms a long-lived phosphorylated intermediate. J Bacteriol 193:3332–3341. https://doi.org/10.1128/JB.00362-11.
26. Li C, Bakker RG, Motaleb MA, Sartakova ML, Cabello FC, Charon NW. 2002. Asymmetrical flagellar rotation in Borrelia burgdorferi nonchemotactic mutants. Proc Natl Acad Sci U S A 99:6169–6174. https://doi.org/10.1073/pnas.092010499.
27. Zhang K, Liu J, Tu Y, Xu H, Charon NW, Li C. 2012. Two CheW coupling proteins are essential in a chemosensory pathway of Borrelia burgdorferi. Mol Microbiol 85:782–794. https://doi.org/10.1111/j.1365-2958.2012.08139.x.

28. Xu H, Raddi G, Liu J, Charon NW, Li C. 2011. Chemoreceptors and flagellar motors are subterminally located in close proximity at the two cell poles in spirochetes. J Bacteriol 193:2652–2656. https://doi.org/10.1128/JB.01530-10.
29. Zhang K, Liu J, Charon NW, Li C. 2015. Hypothetical protein BB0569 is essential for chemotaxis of the Lyme disease spirochete Borrelia burgdorferi. J Bacteriol 198:664–672. https://doi.org/10.1128/JB.00877-15.
30. Pazy Y, Motaleb MA, Guarnieri MT, Charon NW, Zhao R, Silversmith RE. 2010. Identical phosphatase mechanisms achieved through distinct modes of binding phosphoprotein substrate. Proc Natl Acad Sci U S A 107:1924–1929. https://doi.org/10.1073/pnas.0911185107.
31. Motaleb MA, Miller MR, Li C, Bakker RG, Goldstein SF, Silversmith RE, Bourret RB, Charon NW. 2005. CheX is a phosphorylated CheY phosphatase essential for Borrelia burgdorferi chemotaxis. J Bacteriol 187:7963–7969. https://doi.org/10.1128/JB.187.23.7963-7969.2005.
32. Liu J, Lin T, Botkin DJ, McCrum E, Winkler H, Norris SJ. 2009. Intact flagellar motor of Borrelia burgdorferi revealed by cryo-electron tomography: evidence for stator ring curvature and rotor/C-ring assembly flexion. J Bacteriol 191:5026–5036. https://doi.org/10.1128/JB.00340-09.
33. Charon NW, Goldstein SF. 2002. Genetics of motility and chemotaxis of a fascinating group of bacteria: the spirochetes. Annu Rev Genetics 36:47–73. https://doi.org/10.1146/annurev.genet.36.041602.134359.
34. Fosnaugh K, Greenberg EP. 1988. Motility and chemotaxis of Spirochaeta aurantia: computer-assisted motion analysis. J Bacteriol 170:1678–1774.
35. Butler SM, Camilli A. 2005. Going against the grain: chemotaxis and infection in Vibrio cholerae. Nat Rev Microbiol 3:611–620. https://doi.org/10.1038/nrmicro1207.
36. Butler SM, Camilli A. 2004. Both chemotaxis and net motility greatly influence the infectivity of Vibrio cholerae. Proc Natl Acad Sci U S A 101:5018–5023. https://doi.org/10.1073/pnas.0308052101.
37. McGee DJ, Langford ML, Watson EL, Carter JE, Chen YT, Ottemann KM. 2005. Colonization and inflammation deficiencies in Mongolian gerbils infected by Helicobacter pylori chemotaxis mutants. Infect Immun 73:1820–1827. https://doi.org/10.1128/IAI.73.3.1820-1827.2005.
38. Terry K, Williams SM, Connolly L, Ottemann KM. 2005. Chemotaxis plays multiple roles during Helicobacter pylori animal infection. Infect Immun 73:803–811. https://doi.org/10.1128/IAI.73.2.803-811.2005.
39. Lertsethtakarn P, Ottemann KM, Hendrixson DR. 2011. Motility and chemotaxis in Campylobacter and Helicobacter. Annu Rev Microbiol 65:389–410. https://doi.org/10.1146/annurev-micro-090110-102908.
40. Pitzer JE, Sultan SZ, Hayakawa Y, Hobbs G, Miller MR, Motaleb MA. 2011. Analysis of the Borrelia burgdorferi cyclic-di-GMP binding protein PlzA reveals a role in motility and virulence. Infect Immun 79:1815–1825. https://doi.org/10.1128/IAI.00075-11.
41. Stewart PE, Bestor A, Cullen JN, Rosa PA. 2008. A tightly regulated surface protein of Borrelia burgdorferi is not essential to the mouse-tick infectious cycle. Infect Immun 76:1970–1978. https://doi.org/10.1128/IAI.00714-07.
42. Pappas CJ, Iyer R, Petzke MM, Caimano MJ, Radolf J, Schwartz I. 2011. Borrelia burgdorferi requires glycerol for maximum fitness during the tick phase of the enzootic cycle. PLoS Pathog 7:e1002102. https://doi.org/10.1371/journal.ppat.1002102.
43. Rogers EA, Terekhova D, Zhang HM, Hovis KM, Schwartz I, Marconi RT. 2009. Rrp1, a cyclic-di-GMP-producing response regulator, is an important regulator of Borrelia burgdorferi core cellular functions. Mol Microbiol 71:1551–1573. https://doi.org/10.1111/j.1365-2958.2009.06621.x.
44. Dresser AR, Hardy PO, Chaconas G. 2009. Investigation of the genes involved in antigenic switching at the vlsE locus in Borrelia burgdorferi: an essential role for the RuvAB branch migrase. PLoS Pathog 5:e1000680. https://doi.org/10.1371/journal.ppat.1000680.
45. Miller CL, Karna SL, Seshu J. 2013. Borrelia host adaptation regulator (BadR) regulates rpoS to modulate host adaptation and virulence factors in Borrelia burgdorferi. Mol Microbiol 88:105–124. https://doi.org/10.1111/mmi.12171.
46. Purser JE, Norris SJ. 2000. Correlation between plasmid content and infectivity in Borrelia burgdorferi. Proc Natl Acad Sci U S A 97:13865–13870. https://doi.org/10.1073/pnas.97.25.13865.
47. Motaleb MA, Pitzer JE, Sultan SZ, Liu J. 2011. A novel gene inactivation system reveals an altered periplasmic flagellar orientation in a Borrelia burgdorferi fliL mutant. J Bacteriol 193:3324–3331. https://doi.org/10.1128/JB.00202-11.
48. Sultan SZ, Pitzer JE, Miller MR, Motaleb MA. 2010. Analysis of a Borrelia burgdorferi phosphodiesterase demonstrates a role for cyclic-di-guanosine monophosphate in motility and virulence. Mol Microbiol 77:128–142. https://doi.org/10.1111/j.1365-2958.2010.07191.x.
49. Szurmant H, Ordal GW. 2004. Diversity in chemotaxis mechanisms among the bacteria and archaea. Microbiol Mol Biol Rev 68:301–319. https://doi.org/10.1128/MMBR.68.2.301-319.2004.
50. Hyakutake A, Homma M, Austin MJ, Boin MA, Hase CC, Kawagishi I. 2005. Only one of the five CheY homologs in Vibrio cholerae directly switches flagellar rotation. J Bacteriol 187:8403–8410. https://doi.org/10.1128/JB.187.24.8403-8410.2005.
51. Bandyopadhaya A, Chaudhuri K. 2009. Differential modulation of NF-kappaB-mediated pro-inflammatory response in human intestinal epithelial cells by cheY homologues of Vibrio cholerae. Innate Immun 15:131–142. https://doi.org/10.1177/1753425908100454.
52. Kirby JR, Zusman DR. 2003. Chemosensory regulation of developmental gene expression in Myxococcus xanthus. Proc Natl Acad Sci U S A 100:2008–2013. https://doi.org/10.1073/pnas.0330944100.
53. McBride MJ, Weinberg RA, Zusman DR. 1989. "Frizzy" aggregation genes of the gliding bacterium Myxococcus xanthus show sequence similarities to the chemotaxis genes of enteric bacteria. Proc Natl Acad Sci U S A 86:424–428. https://doi.org/10.1073/pnas.86.2.424.
54. Yang Z, Ma X, Tong L, Kaplan HB, Shimkets LJ, Shi W. 2000. Myxococcus xanthus dif genes are required for biogenesis of cell surface fibrils essential for social gliding motility. J Bacteriol 182:5793–5798. https://doi.org/10.1128/JB.182.20.5793-5798.2000.
55. Berleman JE, Bauer CE. 2005. A che-like signal transduction cascade involved in controlling flagella biosynthesis in Rhodospirillum centenum. Mol Microbiol 55:1390–1402. https://doi.org/10.1111/j.1365-2958.2005.04489.x.
56. Berleman JE, Bauer CE. 2005. Involvement of a Che-like signal transduction cascade in regulating cyst cell development in Rhodospirillum centenum. Mol Microbiol 56:1457–1466. https://doi.org/10.1111/j.1365-2958.2005.04646.x.
57. Black WP, Yang Z. 2004. Myxococcus xanthus chemotaxis homologs DifD and DifG negatively regulate fibril polysaccharide production. J Bacteriol 186:1001–1008. https://doi.org/10.1128/JB.186.4.1001-1008.2004.
58. Lee SH, Butler SM, Camilli A. 2001. Selection for in vivo regulators of bacterial virulence. Proc Natl Acad Sci U S A 98:6889–6894. https://doi.org/10.1073/pnas.111581598.
59. Kofoid EC, Parkinson JS. 1988. Transmitter and receiver modules in bacterial signaling proteins. Proc Natl Acad Sci U S A 85:4981–4985. https://doi.org/10.1073/pnas.85.14.4981.
60. Wuichet K, Alexander RP, Zhulin IB. 2007. Comparative genomic and protein sequence analyses of a complex system controlling bacterial chemotaxis. Methods Enzymol 422:1–31.
61. Iyer R, Caimano MJ, Luthra A, Axline D, Jr, Corona A, Iacobas DA, Radolf JD, Schwartz I. 2015. Stage-specific global alterations in the transcriptomes of Lyme disease spirochetes during tick feeding and following mammalian host adaptation. Mol Microbiol 95:509–538. https://doi.org/10.1111/mmi.12882.
62. Elias AF, Stewart PE, Grimm D, Caimano MJ, Eggers CH, Tilly K, Bono JL, Akins DR, Radolf JD, Schwan TG, Rosa P. 2002. Clonal polymorphism of Borrelia burgdorferi strain B31 MI: implications for mutagenesis in an infectious strain background. Infect Immun 70:2139–2150. https://doi.org/10.1128/IAI.70.4.2139-2150.2002.
63. Rego RO, Bestor A, Rosa PA. 2011. Defining the plasmid-encoded restriction-modification systems of the Lyme disease spirochete Borrelia burgdorferi. J Bacteriol 193:1161–1171. https://doi.org/10.1128/JB.01176-10.
64. Casjens S, Palmer N, van Vugt R, Huang WM, Stevenson B, Rosa P, Lathigra R, Sutton G, Peterson J, Dodson RJ, Haft D, Hickey E, Gwinn M, White O, Fraser CM. 2000. A bacterial genome in flux: the twelve linear and nine circular extrachromosomal DNAs in an infectious isolate of the Lyme disease spirochete Borrelia burgdorferi. Mol Microbiol 35:490–516.
65. Motaleb MA, Miller MR, Bakker RG, Li C, Charon NW. 2007. Isolation and characterization of chemotaxis mutants of the Lyme disease Spirochete Borrelia burgdorferi using allelic exchange mutagenesis, flow cytometry, and cell tracking. Methods Enzymol 422:421–437. https://doi.org/10.1016/S0076-6879(06)22021-4.
66. Bono JL, Elias AF, Kupko JJ, III, Stevenson B, Tilly K, Rosa P. 2000. Efficient targeted mutagenesis in Borrelia burgdorferi. J Bacteriol 182:2445–2452. https://doi.org/10.1128/JB.182.9.2445-2452.2000.
67. Frank KL, Bundle SF, Kresge ME, Eggers CH, Samuels DS. 2003. aadA confers streptomycin resistance in Borrelia burgdorferi. J Bacteriol 185:6723–6727. https://doi.org/10.1128/JB.185.22.6723-6727.2003.

68. Jewett MW, Lawrence K, Bestor AC, Tilly K, Grimm D, Shaw P, VanRaden M, Gherardini F, Rosa PA. 2007. The critical role of the linear plasmid lp36 in the infectious cycle of Borrelia burgdorferi. Mol Microbiol 64: 1358–1374. https://doi.org/10.1111/j.1365-2958.2007.05746.x.
69. Karna SL, Prabhu RG, Lin YH, Miller CL, Seshu J. 2013. Contributions of environmental signals and conserved residues to the functions of carbon storage regulator A of Borrelia burgdorferi. Infect Immun 81: 2972–2985. https://doi.org/10.1128/IAI.00494-13.
70. Seemanapalli SV, Xu Q, McShan K, Liang FT. 2010. Outer surface protein C is a dissemination-facilitating factor of Borrelia burgdorferi during mammalian infection. PLoS One 5:e15830. https://doi.org/10.1371/journal.pone.0015830.
71. Mulay VB, Caimano MJ, Iyer R, Dunham-Ems S, Liveris D, Petzke MM, Schwartz I, Radolf JD. 2009. Borrelia burgdorferi bba74 is expressed exclusively during tick feeding and is regulated by both arthropod- and mammalian host-specific signals. J Bacteriol 191:2783–2794. https://doi.org/10.1128/JB.01802-08.
72. Patton TG, Dietrich G, Dolan MC, Piesman J, Carroll JA, Gilmore RD, Jr. 2011. Functional analysis of the Borrelia burgdorferi bba64 gene product in murine infection via tick infestation. PLoS One 6:e19536. https://doi.org/10.1371/journal.pone.0019536.
73. Yang XF, Pal U, Alani SM, Fikrig E, Norgard MV. 2004. Essential role for OspA/B in the life cycle of the Lyme disease spirochete. J Exp Med 199:641–648. https://doi.org/10.1084/jem.20031960.
74. Zhang X, Yang X, Kumar M, Pal U. 2009. BB0323 function is essential for Borrelia burgdorferi virulence and persistence through tick-rodent transmission cycle. J Infect Dis 200:1318–1330. https://doi.org/10.1086/605846.